



LAWRENCE
LIVERMORE
NATIONAL
LABORATORY

UCRL-JRNL-214012

Melting of Xenon to 80 GPa, p-d hybridization, and an ISRO liquid

M. Ross, R. Boehler, P. Soderlind

July 27, 2005

Physical Review Letters

This document was prepared as an account of work sponsored by an agency of the United States Government. Neither the United States Government nor the University of California nor any of their employees, makes any warranty, express or implied, or assumes any legal liability or responsibility for the accuracy, completeness, or usefulness of any information, apparatus, product, or process disclosed, or represents that its use would not infringe privately owned rights. Reference herein to any specific commercial product, process, or service by trade name, trademark, manufacturer, or otherwise, does not necessarily constitute or imply its endorsement, recommendation, or favoring by the United States Government or the University of California. The views and opinions of authors expressed herein do not necessarily state or reflect those of the United States Government or the University of California, and shall not be used for advertising or product endorsement purposes.

Melting of Xenon to 80 GPa, p - d hybridization, and an ISRO liquid

Marvin Ross^{1,2}, Reinhard Boehler¹ and Per Söderlind²

1. *Max Planck Institut für Chemie, 55020 Mainz, Germany*

2. *Lawrence Livermore National Laboratory, Livermore, CA 94551, USA*

Measurements made in a laser heated diamond-anvil cell are reported that extend the melting curve of Xe to 80 GPa and 3350 K. The steep lowering of the melting slope (dT/dP) that occurs near 17 GPa and 2750 K results from the hybridization of the p -like valence and d -like conduction states with the formation of clusters in the liquid having Icosahedral Short-Range Order (ISRO).

The traditional view of the heavier rare gas solids, xenon, krypton and argon, is they are closed shell insulators with a filled s^2p^6 valence band separated by 9-12 eV from an empty d -like conduction band. To a good approximation, the intermolecular interaction can be treated as pair-wise additive using a spherically symmetric exponential-six(\exp -6) potential parameterized to fit experimental data[1]. However, recent high pressure studies show that the crystal structure, and melting curves, of these elements are more complicated than previously believed. While the structure at ambient conditions is fcc there is now experimental evidence for a pressure-induced fcc to hcp transition [2-4]. This transition was first predicted for argon by McMahan using electron band theory[5]. He reported an upper bound of 230 GPa for the transition. The very small energy difference between fcc and hcp makes an accurate prediction of the pressure difficult. McMahan argued that this transition follows from the effects of hybridization between the l -valence and $l+1$ conduction band as the energy gap between the two bands narrow.

High-resolution angle dispersive synchrotron x-ray diffraction experiments have observed the coexistence of fcc and hcp structures in temperature quenched samples of Xe from 1.5 GPa up to 41 GPa[3], Kr from 3.2

to 50 GPa[4a]. Above the upper pressure only the hcp structure is observed. For Ar, fcc and hcp were observed from 30 to 105 GPa, the highest pressure at which measurements were made [4b]. With increasing pressure the valence-conduction band gap decreases, and closes, leading to a metallic-like phase in the hcp structure. Xe becomes metallic at room temperature near 132-150 GPa [6-8]. Kr and Ar are predicted to become metallic near 310[9a,b] and 430-514 GPa[5,9a].

The melting curves have been measured in a laser heated diamond-anvil cell (DAC) to pressures of nearly 40, 60 and 80 GPa for Xe, Kr and Ar respectively[10]. For these solids, a considerable decrease in the melting slope (dT/dP) was observed starting near 17, 30 and 40 GPa. The purpose of this paper is to report new measurements for the xenon melting curve to 80 GPa (3350 K), which doubles the previous pressure range, and to provide evidence that the bend in the melting slope follows from the effects of p - d hybridization due to band gap narrowing.

The experimental method employed here has been described in detail in previous publications [10,11]. A schematic of the diamond cell is shown in figure 1. A 25 W Nd: YAG laser (1.06 mm wavelength) is used to heat a W or Re metal foil. Ideally, the samples should not absorb the laser radiation nor emit incandescent light in detectable amounts. Only the metal foil absorbs laser radiation. As soon as the metal surface reaches the melting temperature of the solid sample, a thin layer in contact with the metal starts to melt. Melting is readily observed with the laser speckle method by the observation of a continuous motion in the laser speckle pattern appearing in the liquid phase upon melting, and disappearing during freezing. Temperatures are measured at the onset of this motion when the temperature was slowly increased or at the disappearance of motion at decreasing temperature. The measured melting and freezing temperatures were within the experimental uncertainty that was estimated from a minimum of five melting-freezing cycles to be ± 100 K. This method for measuring melting temperatures has been extensively tested for alkali halides [11] where the results can be directly compared with low pressure melting data obtained using thermocouples.

The continuous speckle motion observed in a liquid during melting is drastically different from the observed *lack of* motion occurring in a solid. As such, it clearly distinguishes between a solid-liquid and a solid-solid transition, or of a glass-solid transition. Consequently, there is no basis for a recent proposal[12] that the solid-liquid melt curve is an fcc-bcc phase boundary. One can demonstrate this trivially from theory. It is well known that a bcc phase is unstable at all temperatures for inverse power potential ($\sim 1/r^n$) for $n \sim 6,7$ [13]. Since the exp-6 potential[12] used for calculating the Xe melting curve can be approximated by an inverse $n \sim 9,10$ power potential, then a bcc solid Xe phase must be unstable. This conclusion has been reinforced by the recent Monte Carlo simulations of the melting curve by Saija and Prestipino[14], using the same exp-6 potential as in reference [12].

Figure 2 shows the results of our present and earlier Xe melting measurements[10] and those reported by Jephcoat and Besedin [15]. Included in the figure is the melting curve calculated by the principle of corresponding states using the depth and location of the exp-6 energy minimum to scale the melting curves of neon and argon to Xe[16]. The measured melting temperatures rise from ambient with increasing pressure up to about 17 GPa and 2750 K, in agreement with the corresponding states and the measurements of Jephcoat and Besedin. Above this pressure the temperature rises more slowly. From 40 to 80 GPa (3350 K) it flattens, and exhibits a rise of only about 200 K, a $dT/dP \sim 5\text{K/GPa}$. In our earlier paper the melting anomaly was interpreted in terms of a model in which the hcp stacking faults in the fcc lattice acted as solutes in a binary system which lower the melting temperature. Since we are now aware that above 41 GPa Xe is fully hcp[3], then the model must be incorrect because it would predict that the melting should rise back up to the corresponding states curve at that pressure.

In the earlier paper total energy calculations were reported for several close-packed structures of xenon: fcc, dhcp, hcp and bcc, using the full-potential linear muffin-tin orbital (FP-LMTO) method[10]. As a part of these calculations d -electron populations were also generated, and are plotted in figure 3. The total d -electron population includes contributions from the filled $4d$ band (10 electrons)

and additional contributions from hybridization between the $5p$ valence and the $5d$ states conduction band. At equilibrium pressure the $4d$ contribution are essentially all core states, but are included in the calculations to insure for better numerical treatment at compressed volumes. Some of the d -band contribution will, for technical reasons, leak out of the muffin-tins spheres and be part of the charge in the so-called interstitial region together with s and p electrons. In this region the electrons cannot be distinguished from each other.

The d -electron population contribution to the $5p$ -like valence band increases with increasing pressure due to hybridization as the gap narrows and closes. Near 17 GPa, the pressure at which the melting curve begins to flatten, the d -population of the valence band has risen to about 0.13 electrons/atom. The electron configuration of the band is effectively $s^2p^{5.87}d^{0.13}$, and neither the atom nor the inter-atomic potential can now be treated as spherically symmetric. Above 17 GPa, the d -population continues to rise and the exp-6 potential is inadequate.

Since we know that the insulator-metal transition is due to the narrowing and closing of the valence-conduction band gap, we might expect that if the bending of the melting curves were also a consequence of the increasing d -character then the pressures at which bending is observed in the heavy gases should scale with the transition pressures. Figure 4 shows that there is a strong linear relationship between the observed "bend" pressures and the transition pressures for observed for Xe, and calculated for Kr and Ar[5,9a,b]. The strong linear correlation between the bend and metal transition pressures confirms the likelihood that hybridization plays an important role in shaping the melting curves. The fcc-hcp transition pressures exhibit the same trend. While this reinforces our conclusions, the uncertainties in the transition pressure determination from quenching, stacking faults and thermal barriers make a quantitative comparison less useful.

Some understanding of a possible physical basis for the lowering of the melting curve can be drawn from the fact that p - d hybridization is in effect a continuous pressure-induced transition from 3-fold to 5-fold symmetry. The creation of five-fold symmetric d -character to the electron charge density

energetically favors structures with Icosahedral Short-Range Order (ISRO) [17]. In contrast to the traditional picture of liquid structures based on a dense random packing of hard spheres or rare gas atoms, Frank[18] was the first to suggest that structures of liquid melts could be based on packings of icosahedral clusters consisting of 13 atoms, 12 atoms with 5-fold symmetry surrounding a central atom[17]. Frank pointed out that an icosahedral cluster of 13 Lennard-Jones atoms has an energy that is 8.4% lower than a close-packed arrangement. Calculations by Xie et al.[19a], using an Ar potential, found the total binding energy an icosahedral structure remains lower than hcp or fcc for clusters of less than 13 shells (8217 atoms). Experimentally, Danylchenko et al., in an electron-diffraction study found the existence of free Ar clusters with $N \sim 600-800$ atoms/cluster[19b].

Although it is impossible to create a crystalline structure in which each atom has 5-fold symmetry, randomly packed ISRO clusters of varying sizes may evolve continuously and be interconnected throughout the liquid[20]. In contrast to the solid in which, despite a small degree of d -like character, the strong repulsive forces stabilize the symmetric close-packed structure, the absence of long-range order allows the liquid greater flexibility to lower its energy by forming locally five-fold icosahedral structures. This is the liquid state analogue of the Jahn-Teller effect by which a system can be stabilized by a structural distortion. As a result, a fractional presence of ISRO's will reduce the average liquid energy and increase the mixing entropy relative to a hard sphere-like liquid, thereby lowering the melting temperature. Above 17 GPa, the pressure-induced narrowing of the band gap increases the degree of p to d -hybridization. The d -population continues to rise, increasing the fraction of ISRO and size of the clusters, thereby maintaining a low melting slope. In the case of transition metals, the low melting slopes determined experimentally have been attributed to the presence of partially filled d -electron valence bands [21-23].

Evidence for the presence of ISRO clustering in stable and under-cooled melts of transition metals at ambient conditions have been reported by Schenk et al.[24] and Lee et al.[25] using neutron scattering and *in situ* x-ray diffraction

methods, respectively. Among these metals are Ni, Fe, Zr[24], Fe, Ti [25]. First principles molecular dynamics simulations made by Jaske et al. [26] found evidence for the existence of short range order in the stable and under-cooled melts of Ni, Zr, and Ta. Although ISRO has not been investigated in liquid metals at elevated pressures it is highly likely that these structures will persist.

The p to d -hybridization in the rare gases and the s - d transition in metals have the same physical origin. In the case of metals, for example Cs, increasing pressure broadens the $5s$ -like valence band relative to the unoccupied $5d$ -levels and leads to an overall increase in d -character. At much higher compression, the narrowing energy gap separating the $5s$ - d valence band and the inner $4p$ -core band drives the stabilization of new more open structures [27,28]. In the case of Xe, it is the empty $5d$ -conduction band that hybridizes with the filled $5p$ -valence band driving the fcc-hcp transition[5] that destroys the rare gas sphericity of the interatomic potential by introducing d -like character.

Roughly speaking, the bend in the melting curve near 17 GPa may be considered a triple point connecting the close-packed solid, the hard-sphere-like liquid at lower pressure and the liquid ISRO at higher pressure. The smooth curvature of the melting curve indicates that the hard-sphere-like to SIRO liquid-liquid transition is continuous. Since the ISRO has a solid-like density, then $dT/dP \sim 0$. All of this is due to symmetry breaking of the inter-atomic potential created by the p - d hybridization. The shift from fcc to hcp has a minimal effect on the free energy. The role of hybridization and its influence on the solid-liquid transition has broader implications.

Acknowledgments – We wish to thank Mikhail Erements, Daniel Errandonea, and Andy McMahan for helpful comments. The work was partially supported under the auspices of the U.S. Department of Energy by the University of California Lawrence Livermore National Laboratory under contract No. W-7405-ENG-48.

References

1. M. Ross and A.K. McMahan, *Phys. Rev. B* **21**, 1658 (1980).
2. A.P. Jephcoat, H.-k. Mao, L.W. Finger, D.E. Cox, R.J. Hemley and C.-s. Zha, *Phys. Rev. Lett.*, **59**, 2670 (1987).
3. H. Cynn, C-S. Yoo, B. Baer, V. Iota-Herbei, A.K. McMahan, M. Nicol and S. Carlson, *Phys. Rev. Lett.* **86**, 4552 (2001); H. Cynn and C-S. Yoo, *Phys. Rev. Lett.* **86**, 5731 (2001).
- 4a. D. Errandonea, B. Schwager, R. Boehler and M. Ross, *Phys. Rev. B* **65**, 214110 (2002).
- 4b. D. Errandonea, personal communication.
5. A.K. McMahan, *Phys. Rev. B* **33**, 5344(1986).
6. R.Reichlin, K.E. Brister, A.K. McMahan, M.Ross, S.Martin, Y.K. Vohra and A.L. Ruoff, *Phys. Rev. Lett.* **62**, 669 (1989).
7. K.A. Goettel, J.H. Eggert and I.F. Silvera, *Phys. Rev. Lett.* **62**, 665 (1989).
8. M. I. Eremets, E. Gregoryanz, V.V. Struzhkin, H-k Mao and R.J. Hemley, *Phys. Rev. Lett.* **85**, 2797 (2000).
- 9a. I. Kwon, L.A. Collins, J.D. Kress and N. Troullier, *Phys. Rev. B* **52**, 15165 (1995).
- 9b. J. Hama and K. Suito, *Phys. Lett. A* **140**,117(1989).
10. R. Boehler, M. Ross, P. Söderlind, D.B. Boercker, *Phys. Rev. Lett.* **86**, 5731 (2001).
11. R. Boehler, M. Ross, and D. B. Boercker, *Phys. Rev. Lett.* **78**, 4589 (1997).
12. A. B. Belonoshko, R. Ahuja, and B. Johansson, *Phys. Rev. Lett.* **87**, 165505 (2001). A. B. Belonoshko, O. LeBacq, R. Ahuja, and B. Johansson, *J. Chem. Phys.* **117**,7233 (2002).
13. D. H. E. Dubin and H. Dewitt, *Phys. Rev. B* **49**, 3043 (1994).
14. F. Saija and S. Prestipino, private communication.
15. A. P. Jephcoat and S. Besedin, in *US-Japan Conference in Mineral Physics*, edited by M. Manghnani and T. Yagi (AGU Publications, Washington,DC, 1997).
16. W.L. Vos, J.A. Schouten, D.A. Young, and M. Ross, *J. Chem. Phys.* **94**, 3835 (1991).
17. A.L. MacKay, *Acta Crystallogr.* **15**, 916 (1962).
- 18 F.C. Frank, *Proc. R. Soc. London*, **Ser. A** **215**, 43 (1952).
- 19a J. Xie, J.A. Northby, D.L. Freeman and J.D. Doll, *J. Chem Phys.* **91**, 612(1989).
- 19b. O.G. Danylchenko, S.I. Kovalenko, and V.N Samovarov, *Low Temp. Phys.* **30**, 743(2004).

- 20 H. Jónsson and H.C. Anderson, *Phys. Rev. Lett.* **60**, 2295 (1988).
21. D. Errandonea, B. Schwager, R. Ditz, R. Boehler, and M. Ross, *Phys. Rev. B* **63**, 132104 (2001).
22. M. Ross, L.H. Yang, and R. Boehler, *Phys. Rev. B*, **70**, 184112 (2004).
23. S. Japel, R. Boehler, B. Schwager, and M. Ross, *Phys. Rev. Lett.*, in press.
24. T. Schenk, D. Holland-Moritz, V. Simonet, R. Bellissent, and D.M. Herlach, *Phys. Rev. Lett.* **89**, 075507 (2002).
25. G.W. Lee, A.K. Gangopadhyay, K.F. Kelton, R.W. Hyers, T.J. Rathz, J.R. Rogers, and D.S. Robinson, *Phys. Rev. Lett.* **93**, 1982 (2004).
26. N. Jakse and A. Pasturel, *J.Chem.Phys.***120**, 6124(2004);N. Jakse and A. Pasturel, *Phys. Rev. Lett.* **91**, 195501(2003); N. Jakse, O. Le Bacq, and A. Pasturel, *Phys. Rev.B.***70**, 174203(2004).
27. A.K. McMahan, *Phys. Rev. B* **29**, 5982 (1984).
28. R. Ahuja, P. Soderlind, J.Trygg, J. Melsen, J.M. Wills, B. Johansson and O. Ericksson, *Phys. Rev. B* **50**, 14690 (1994).

Figure Captions

Fig. 1 Schematic diagram of the laser heated diamond-anvil cell (DAC).

Fig. 2 Xe melting curve. Data reported here and in reference [10] (filled circles). Jephcoat and Besedin[13] (empty circles). Corresponding states (solid curve)

Fig. 3 Calculated *d*-electron population.

Fig. 4 Melting "bend" pressure versus the insulator-metal transition pressures. A nominal error of $\pm 10\%$ was chosen for the uncertainty of the data. References to the plotted data are provided in the text.

Fig.1

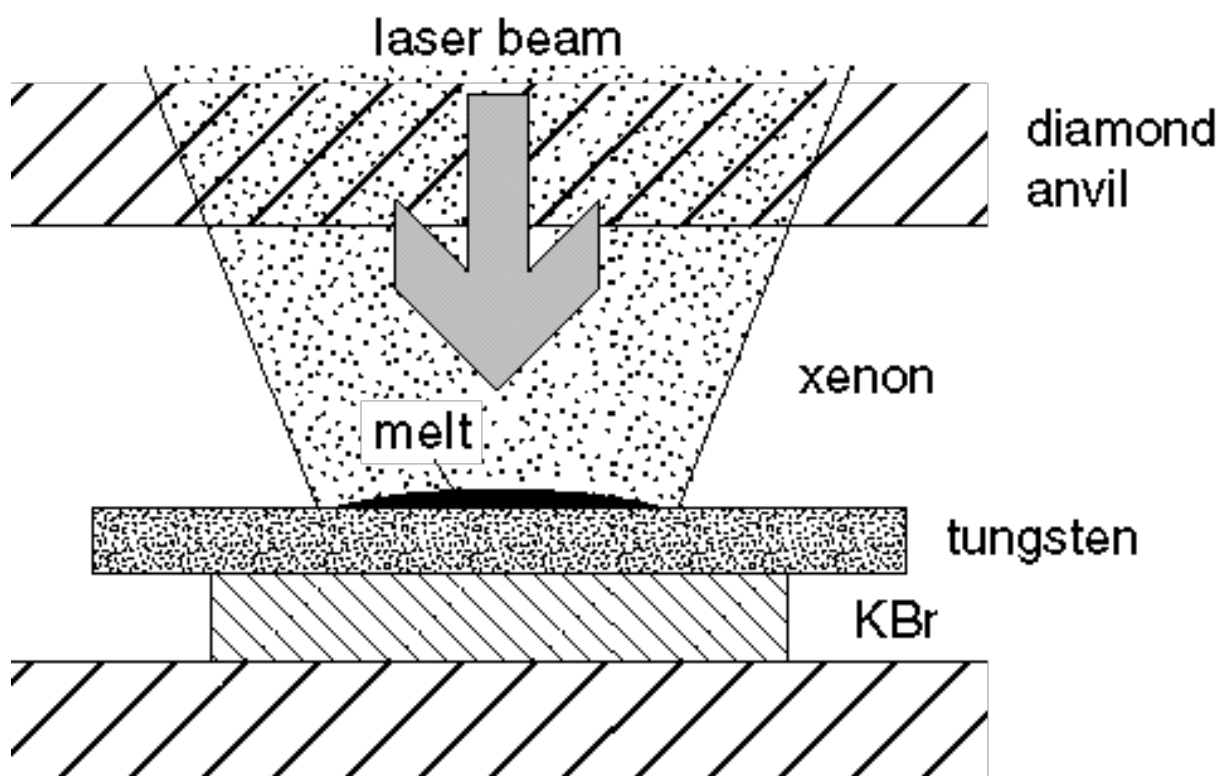


Fig 2

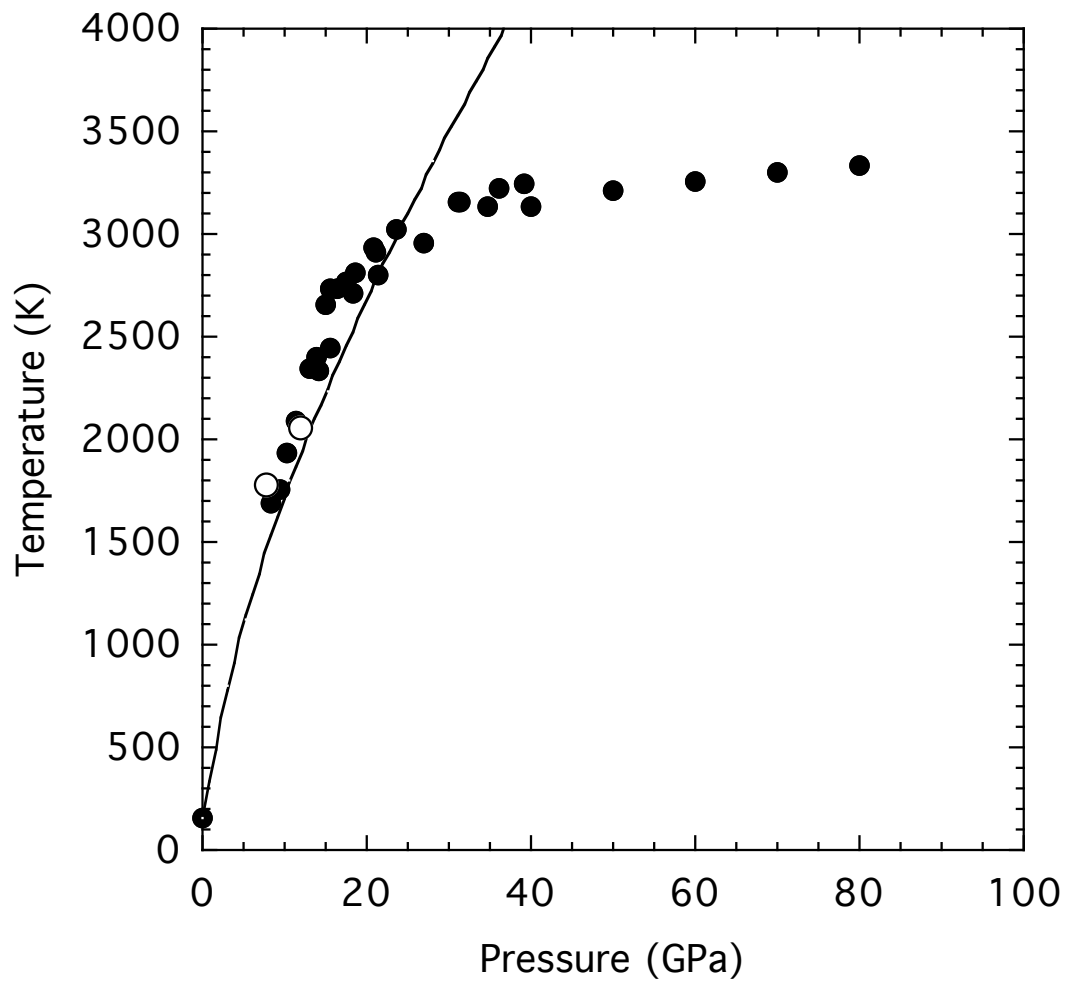


Fig. 3

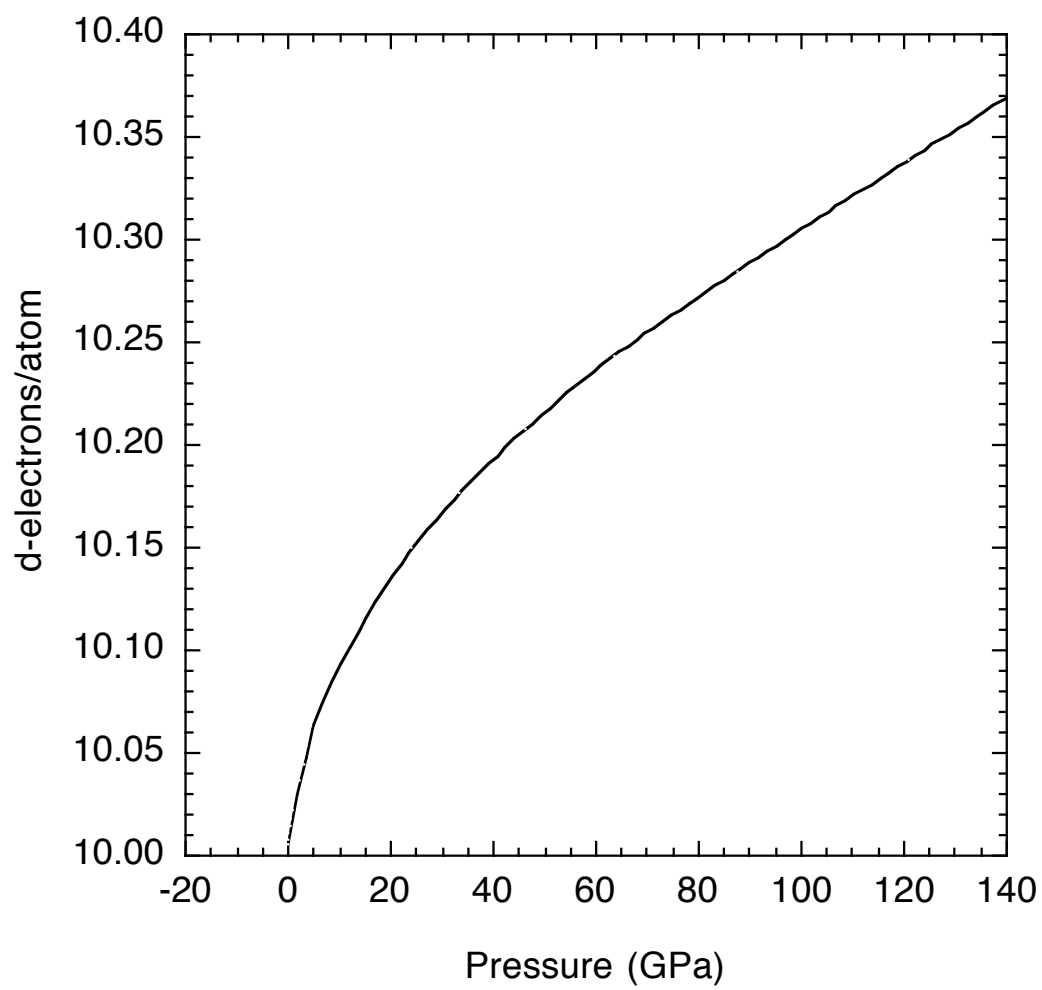


Fig. 4

